

Thermodynamic efficiency of atmospheric motion governed by Lorenz system

Li Zhen* and Yuki Izumida†

*Department of Complexity Science and Engineering, Graduate School of Frontier Sciences,
The University of Tokyo, Kashiwa 277-8561, Japan.*

We formulate the thermodynamic efficiency of convective atmospheric motion governed by the Lorenz system by considering it a non-equilibrium thermodynamic system. The necessary work to maintain atmospheric motion and heat fluxes at the boundaries were calculated. The results show that the efficiency tends to increase as the atmospheric motion is driven far from thermodynamic equilibrium when the Rayleigh number increases. However, it is shown that the efficiency is upper bounded by the maximum efficiency, which is expressed in terms of parameters characterizing the fluid and the convective system. It is also found that there exists an abrupt drop in efficiency at the critical Hopf bifurcation point, leading to chaotic dynamics from stationary ones. These properties are similar to those found previously in Malkus-Lorenz waterwheel system.

I. INTRODUCTION

Understanding atmospheric motion constitutes an important element for understanding the complex climate system. The atmospheric motions on all scales are primarily driven by thermal inequalities owing to solar heating [1]. Historically, Saltzman demonstrated a simplified model of time-dependent convective motion and primarily solved it using Fourier expansion in 1962 [1]. Based on Saltzman's model, Lorenz derived a set of nonlinear ordinary differential equations, known as Lorenz equations, describing the motion of a specific mode of atmosphere and discussing the stability [2].

The Lorenz equations are well known for yielding chaotic solutions under certain parameters and initial conditions. In addition to atmospheric motion, Lorenz equations can be applied in different areas, such as DC motors [3] and chemical reactions [4]. Meanwhile, a mechanical waterwheel model, known as the Malkus-Lorenz wheel, is (partly) governed by the Lorenz equations [5–7].

From the viewpoint of fundamental physics, atmospheric motion can be regarded as a nonequilibrium thermodynamic system that balances the input and output of energy and entropy with the surroundings [8–11]. This viewpoint allows us to regard the atmospheric system as a heat engine driven by temperature differences [10, 12, 13]. The atmospheric motion can be interpreted as the result of mechanical work dissipated by viscosity and as a way to re-equilibrate the energy balance by heat transport [10, 14, 15]. Johnson obtained a Carnot heat-engine-equivalent picture by defining heat reservoirs and their temperature robustly [16]. The impacts of global warming on the thermodynamics of the climate, including thermodynamic efficiency, were studied using a simplified yet Earth-like climate model with the variation of the CO₂ concentration [8].

For the Lorenz equations, the thermodynamic efficiency is numerically calculated and discussed in the

Malkus-Lorenz wheel system [7]. It is bounded by the maximum efficiency and shows an abrupt drop at the point where the dynamics change from stationary to chaotic [7]. In this study, stimulated by [7], the thermodynamic efficiency of atmospheric motion is studied based on Saltzman's model and Lorenz equations. Considering the mathematical similarity, it can be reasonably assumed that this efficiency is similar to those in [7].

The remainder of this paper is structured as follows: A review of the setup of the Lorenz system is given in Sec. II. Subsequently, the thermodynamic efficiency of atmospheric motion is calculated in Sec. III. To obtain efficiency, the heat flux and work necessary to maintain the atmospheric motion are determined. Then in Sec. IV, a numerical calculation of efficiency is applied for one set of parameters, which can lead to chaotic dynamics with a relatively high Rayleigh number. Finally, we summarize the present study and discuss it in Sec. V.

II. LORENZ SYSTEM

First, we review the setup of the Lorenz system [1, 2]. It was originally derived from the Oberbeck-Boussinesq approximation of fluid conservation equations, where the density variations are neglected, except when they give rise to a gravitational force [12]. Let us consider the atmospheric motion between two parallel horizontal plates with distance H , where each plate is externally heated to maintain its temperature such that the temperature difference ΔT between the plates is maintained constant. Assuming that the atmospheric motion is restricted to a two-dimensional x - z plane with vanishing velocity in y -direction, the Navier-Stokes equations and thermal convection equation in x - z plane under the Oberbeck-Boussinesq approximation can be given as follows [1]:

$$\begin{aligned} \frac{\partial v_x}{\partial t} + v_x \frac{\partial v_x}{\partial x} + v_z \frac{\partial v_x}{\partial z} + \frac{\partial P}{\partial x} - \nu \nabla^2 v_x &= 0, \\ \frac{\partial v_z}{\partial t} + v_x \frac{\partial v_z}{\partial x} + v_z \frac{\partial v_z}{\partial z} + \frac{\partial P}{\partial z} - g\alpha T - \nu \nabla^2 v_z &= 0, \end{aligned} \quad (1)$$

* li-zhen@g.ecc.u-tokyo.ac.jp

† izumida@k.u-tokyo.ac.jp

$$\frac{\partial T}{\partial t} + v_x \frac{\partial T}{\partial x} + v_z \frac{\partial T}{\partial z} - \kappa \nabla^2 T = 0. \quad (2)$$

Here, v_x and v_z are the velocities in x - and z -directions, respectively, satisfying the incompressibility condition $\frac{\partial v_x}{\partial x} + \frac{\partial v_z}{\partial z} = 0$ in x - z plane. T and P are the temperature and pressure divided by density, respectively. The constants g , α , ν , and κ denote the acceleration due to gravity, coefficient of thermal expansion, kinematic viscosity, and thermal conductivity, respectively.

Owing to the incompressibility condition, the stream function ψ can be introduced for two-dimensional motion, where the velocities in x - and z -directions are expressed as $v_x = -\frac{\partial \psi}{\partial z}$ and $v_z = \frac{\partial \psi}{\partial x}$, respectively. We also introduce θ , which is the nonlinear part of temperature T :

$$T = T_h - \frac{\Delta T}{H} z + \theta, \quad (3)$$

which also denotes the departure of temperature from that in a state of vanishing convection [2], where $T_h \equiv T|_{z=0}$. Then, the governing equations (1) and (2) can be rewritten in terms of ψ and θ as [1]

$$\frac{\partial}{\partial t} \nabla^2 \psi + \frac{\partial(\psi, \nabla^2 \psi)}{\partial(x, z)} - \nu \nabla^4 \psi - g\alpha \frac{\partial \theta}{\partial z} = 0, \quad (4)$$

$$\frac{\partial}{\partial t} \theta + \frac{\partial(\psi, \theta)}{\partial(x, z)} - \frac{\Delta T}{H} \frac{\partial \psi}{\partial x} - \kappa \nabla^2 \theta = 0, \quad (5)$$

where

$$\frac{\partial(a, b)}{\partial(x, z)} \equiv \left(\frac{\partial a}{\partial x} \frac{\partial b}{\partial z} - \frac{\partial a}{\partial z} \frac{\partial b}{\partial x} \right) \quad (6)$$

is the Jacobian operator

Using the method developed in [17] by scaling the length in H , time in H^2/κ , stream function in κ , and temperature in $(\kappa\nu)/(g\alpha H^3)$, a dimensionless version of Eqs. (4) and (5) can be given as

$$\frac{\partial}{\partial t^*} \nabla^{*2} \psi^* + \frac{\partial(\psi^*, \nabla^{*2} \psi^*)}{\partial(x^*, z^*)} - \sigma \nabla^{*4} \psi^* - \sigma \frac{\partial \theta^*}{\partial z^*} = 0, \quad (7)$$

and

$$\frac{\partial}{\partial t^*} \theta^* + \frac{\partial(\psi^*, \theta^*)}{\partial(x^*, z^*)} - R \frac{\partial \psi^*}{\partial x^*} - \nabla^{*2} \theta^* = 0, \quad (8)$$

with Prandtl number $\sigma \equiv \nu/\kappa$ and Rayleigh number $R \equiv (g\alpha H^3 \Delta T)/(\kappa\nu)$. Here, superscript “*” denotes the dimensionless replacement of the corresponding variable.

Naturally, for both the upper and lower boundaries, we impose

$$\theta^*|_{z^*=0,1} = 0 \quad (9)$$

because the temperatures of the two parallel horizontal plates are maintained constant. Moreover, we impose the

following free boundary conditions on ψ^* for tractability [2]:

$$\begin{aligned} \psi^*|_{z^*=0,1} &= 0, \\ \nabla^{*2} \psi^*|_{z^*=0,1} &= 0. \end{aligned} \quad (10)$$

By considering the boundary conditions Eqs. (9) and (10), modes $\cos(m\pi ax^*) \sin(n\pi z^*)$ and $\sin(m\pi ax^*) \sin(n\pi z^*)$ are available for θ^* and ψ^* , where a^{-1} is the dimensionless wavelength in x -direction, and m and n are the wave numbers in x - and z -directions, respectively.

Lorenz discovered that for a specific set of modes,

$$\begin{aligned} a(1+a^2)^{-1} \psi^* &= X \sqrt{2} \sin(\pi ax^*) \sin(\pi z^*), \\ \pi R_c^{-1} \theta^* &= Y \sqrt{2} \cos(\pi ax^*) \sin(\pi z^*) - Z \sin(2\pi z^*), \end{aligned} \quad (11)$$

where

$$R_c \equiv \pi^4 (1+a^2)^3 a^{-2}, \quad (12)$$

denotes the critical Rayleigh number, X , Y and Z are governed by the following equations.

$$\begin{aligned} \frac{dX}{d\tau} &= -\sigma X + \sigma Y, \\ \frac{dY}{d\tau} &= -XZ + rX - Y, \\ \frac{dZ}{d\tau} &= XY - bZ, \end{aligned} \quad (13)$$

where $\tau \equiv \pi^2(1+a^2)t^*$, $r \equiv R/R_c$, and $b \equiv 4(1+a^2)^{-1}$ [2]. Equation (13) is known as the Lorenz equation. One stable fixed point exists in Eqs. (13),

$$X = Y = Z = 0, \quad (14)$$

when $0 < r < 1$ and three fixed points

$$X = Y = Z = 0, \quad (15)$$

$$X = Y = \pm \sqrt{b(r-1)}, \quad Z = r-1, \quad (16)$$

when $r > 1$ [2]. For $r > 1$, fixed point (15) is unstable, whereas fixed points (16) are stable if $0 < \sigma < b+1$ [2]. However, if $\sigma > b+1$, fixed points (16) are unstable when $r > \sigma(\sigma+b+3)/(\sigma-b-1)$ and the strange attractor called “Lorenz attractor” appears [2]. A pitchfork bifurcation occurs at $r = 1$, and if $\sigma > b+1$, a subcritical Hopf bifurcation occurs at $r = \sigma(\sigma+b+3)/(\sigma-b-1)$ [5]. It can be proven that $\sigma(\sigma+b+3)/(\sigma-b-1) > 1$ for any available b when $\sigma > b+1$.

A mechanical waterwheel model is (partly) governed by the Lorenz equations known as the Malkus-Lorenz wheel, in which water flows into a sloping wheel in a symmetry mode and leaks at a constant rate, causing the wheel to rotate against friction [5–7]. This waterwheel model can be regarded as a generalized heat engine

because it absorbs potential energy from the inflow and works against friction to maintain its rotation [7]. The thermodynamic efficiency is given by

$$\eta = \eta_{\max} \left(1 - \frac{1}{r} \right), \quad (17)$$

when the system approaches stable fixed points (16) and is bounded by the maximum efficiency η_{\max} irrespective of whether the dynamic is chaotic [7]. r is the redefined Rayleigh number in the waterwheel model.

The thermodynamic efficiency of the Malkus-Lorenz wheel is related to the Rayleigh number, which, in the atmospheric motion situation, is related to the temperature difference ΔT . Similar to the Malkus-Lorenz wheel, it is also necessary for the atmosphere to absorb energy, particularly heat energy, to maintain its motion. Thus, it is reasonable to regard atmospheric motion as a heat engine and the thermodynamic efficiency, which may also be bounded by maximum efficiency, can be expressed by the Rayleigh number R . That is, the efficiency may be similar to Eq. (17) when dynamics are stationary.

Moreover, the thermodynamic efficiency of free convection is qualitatively given as:

$$\eta \sim \frac{g\alpha L}{C_p}, \quad (18)$$

where L is the length scale of the convection system (for the situation considered in this study, H) and C_p is the constant-pressure specific heat [12]. This expression may be related to maximum efficiency η_{\max} .

Thus, it is natural to assume that the efficiency studied here is a combination of Eq. (17), and Eq. (18).

III. THERMODYNAMIC EFFICIENCY

Figure 1 shows a schematic of atmospheric motion. The heat \dot{Q}_{in} is absorbed per unit time at the hot boundary $z = 0$, and a part of it is converted to work per unit time \dot{W} to maintain the motion. The heat \dot{Q}_{out} is dissipated per unit time at the cold boundary $z = H$. The efficiency can be defined as:

$$\eta \equiv \frac{\dot{W}}{\dot{Q}_{\text{in}}}. \quad (19)$$

Note that \dot{W} is usually dissipated again, such that $\dot{Q}_{\text{in}} \approx \dot{Q}_{\text{out}}$ [12].

Moreover, it is necessary to revert to the governing equations (1) and (2) before calculating heat absorbed per unit time \dot{Q}_{in} , which is related to heat flux \mathbf{j} , and work per unit time \dot{W} .

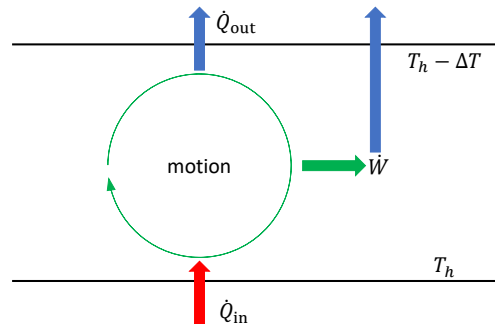


FIG. 1. Illustration of the atmospheric motion when it is regarded as a heat engine. Heat is absorbed at the hot boundary ($z = 0$ with temperature T_h) as \dot{Q}_{in} (red bold arrow), and dissipated at the cold boundary ($z = H$ with temperature $T_h - \Delta T$) as \dot{Q}_{out} (blue bold arrows). A part of the heat absorbed is converted to the necessary work \dot{W} (green bold arrow) to maintain the motion (green ring arrow). However, this work is usually dissipated again [12].

A. Heat flux

It is easy to obtain the heat flux $\mathbf{j} = (j_x, j_z)$ that satisfies

$$\frac{\partial T}{\partial t} + \nabla \cdot \mathbf{j} = 0 \quad (20)$$

from Eq. (2) with incompressibility condition in x - z plane. Here, \mathbf{j} can be chosen as

$$\mathbf{j} = \mathbf{v}T - \kappa \nabla T, \quad (21)$$

which is the total heat flux including convection term $\mathbf{v}T$ where $\mathbf{v} = (v_x, v_z)$ and conduction term $-\kappa \nabla T$ [1]. In particular, in z -direction, we have

$$j_z = v_z T - \kappa \frac{\partial T}{\partial z} = \frac{\partial \psi}{\partial x} T - \kappa \frac{\partial T}{\partial z}. \quad (22)$$

j_z at the boundary is related to the absorbed and dissipated heat, respectively. By applying the mode in Eq. (11) and integrating j_z at both the hot boundary $(\partial V)_h = \{(x, z) | z = 0, 0 < x < Ha^{-1}\}$ and the cold boundary $(\partial V)_c = \{(x, z) | z = H, 0 < x < Ha^{-1}\}$, the absorbed heat per unit time can be calculated as follows:

$$\dot{Q}_{\text{in}} = \rho C_p \int_{(\partial V)_h} j_z dx = \rho C_p \frac{\kappa^2 \nu}{ga\alpha H^3} (R + 2R_c Z), \quad (23)$$

whereas the dissipated heat per unit time is

$$\dot{Q}_{\text{out}} = \rho C_p \int_{(\partial V)_c} j_z dx = \rho C_p \frac{\kappa^2 \nu}{ga\alpha H^3} (R + 2R_c Z). \quad (24)$$

Here, $\dot{Q}_{\text{in}} = \dot{Q}_{\text{out}}$, which implies that the work per unit time \dot{W} to maintain the motion is finally dissipated.

B. Work to maintain the atmospheric

motion The kinetic energy per unit mass is defined as follows:

$$e_K \equiv \frac{1}{2} (v_x^2 + v_z^2). \quad (25)$$

Combined with Eq. (1), the energy conservation equation can be expressed as follows:

$$\frac{\partial e_K}{\partial t} = \nu \mathbf{v} \cdot (\nabla^2 \mathbf{v}) + g\alpha v_z T - \nabla \cdot [(e_K + P)\mathbf{v}]. \quad (26)$$

Here, $\nu \mathbf{v} \cdot (\nabla^2 \mathbf{v})$ is related to the necessary work per unit time to maintain the motion, $-\nabla \cdot [(e_K + P)\mathbf{v}]$ is the convection term with no energy input and output, as $[(e_K + P)v_z]|_{z=0,H} = 0$ when considering the boundary conditions (9) and (10), and $g\alpha v_z T$ can be expressed by an ‘‘available potential energy’’ $-(g\alpha H\theta^2)/(2\Delta T)$ when considering the average over the entire fluid [1].

Considering the mode in Eq. (11), the necessary work per unit time \dot{W} to maintain the motion can be calculated by integrating $-\rho\nu \mathbf{v} \cdot (\nabla^2 \mathbf{v})$ over the entire motion space $V = \{(x, z) | 0 < x < Ha^{-1}, 0 < z < H\}$ as

$$\dot{W} = -\rho\nu \int_V \mathbf{v} \cdot (\nabla^2 \mathbf{v}) dV = \frac{2\kappa^2 \nu \rho R_c}{abH^2} X^2. \quad (27)$$

C. Efficiency

It appears that by using \dot{Q}_{in} in Eq. (23) and \dot{W} in Eq. (27), the thermodynamic efficiency can be calculated directly using Eq. (19). However, these dynamics may become chaotic under certain parameter sets. Thus, it is necessary to determine whether the dynamics are stationary or chaotic to obtain efficiency.

The case is straightforward if the dynamics approach a fixed point. Using Eqs. (23) and (27), the efficiency can be expressed as

$$\eta = \frac{\dot{W}}{\dot{Q}_{in}} = \frac{g\alpha H}{C_p} \frac{2R_c X^2}{b(R + 2R_c Z)} \quad (\text{stationary dynamics}). \quad (28)$$

The fixed point (15) is approached if $0 < R/R_c < 1$, whereas the fixed points (16) is approached if $R/R_c > 1$ and $0 < \sigma < b+1$, or if $1 < R/R_c < \sigma(\sigma+b+3)/(\sigma-b-1)$ and $\sigma > b+1$. Thus, the efficiency can be calculated as:

$$\eta = \begin{cases} 0 & (\text{stable fixed point (15)}), \\ \frac{g\alpha H}{C_p} \frac{2(R-R_c)}{3R-2R_c} & (\text{stable fixed points (16)}). \end{cases} \quad (29)$$

For chaotic dynamics, if $R/R_c > \sigma(\sigma+b+3)/(\sigma-b-1)$ and $\sigma > b+1$, it cannot be derived as a closed expression for efficiency because the dynamics evolve through the chaotic attractor [7]. Nevertheless, \dot{W} and \dot{Q}_{in} can be averaged because the limit set is densely covered by a

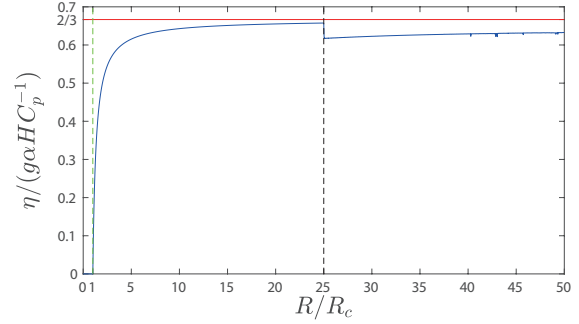


FIG. 2. $\eta/(g\alpha HC_p^{-1})$ vs. R/R_c . Parameters for the corresponding Lorenz equations Eq. (13) are chosen as $b = 2$ and $\sigma = 5$. Pitchfork bifurcation occurs at $R/R_c = 1$ (green dashed line), and subcritical Hopf bifurcation occurs at $R/R_c = \sigma(\sigma + b + 3)/(\sigma - b - 1) = 25$ (black dashed line) [5–7]. $\eta/(g\alpha HC_p^{-1})$ (blue solid line) is bounded by $2/3$ (red solid line) irrespective of whether the dynamics are stable ($R/R_c < 25$) or chaotic ($R/R_c > 25$). However, there is an abrupt drop at $R/R_c = 25$, where the dynamics start to become chaotic. We used the fourth Runge-Kutta method for the numerical calculation.

particular trajectory [7]. The average of a function f is defined as follows:

$$\langle f \rangle \equiv \lim_{\tau \rightarrow +\infty} \frac{1}{\tau} \int_0^\tau f dt. \quad (30)$$

Thus, the efficiency can be expressed as

$$\eta = \frac{\langle \dot{W} \rangle}{\langle \dot{Q}_{in} \rangle} = \frac{g\alpha H}{C_p} \frac{2R_c \langle X^2 \rangle}{b(R + 2R_c \langle Z \rangle)} \quad (\text{chaotic dynamics}). \quad (31)$$

IV. NUMERICAL CALCULATION

Equation (29) shows that the efficiency is bounded by $(2g\alpha H)/(3C_p)$ as R increases when the dynamics are stationary, for example, $0 < \sigma < b+1$. Although the expression of the efficiency cannot be derived as a closed one under chaotic dynamics, it is reasonable to assume that the efficiency shares the same upper bound, $(2g\alpha H)/(3C_p)$, as in the case of stationary dynamics.

Figure 2 shows the numerical calculation results of the non-dimensionalized efficiency $\eta/(g\alpha HC_p^{-1})$, plotted as a blue solid line. The necessary parameters were chosen as $b = 2$ and $\sigma = 5$, making it possible for the dynamics to become chaotic. The two dashed lines in the figure represent the pitchfork bifurcation point at $R/R_c = 1$ (green dashed line) and subcritical Hopf bifurcation point $R/R_c = \sigma(\sigma + b + 3)/(\sigma - b - 1) = 25$ (black dashed line). The stable fixed point (15) is approached when $0 < R/R_c < 1$ and the efficiency vanishes, whereas a stable fixed point (16) is approached when $1 < R/R_c < 25$.

The efficiency is described by Eq. (29) in stationary dynamics and is calculated using Eq. (31), when in chaotic dynamics.

Except for the discontinuous point at $R/R_c = 25$, the efficiency increases as R/R_c increases when $R/R_c > 1$. Because $R \propto \Delta T$, the efficiency increases as the temperature difference increases. This type of behavior is commonly observed in the efficiency of heat engines operating between two heat reservoirs at different temperatures, such as the Carnot heat engine [7].

Moreover, regardless of whether stationary or chaotic, $\eta/(g\alpha HC_p^{-1})$ is bounded by $2/3$ (red solid line), implying that

$$\eta < \frac{2g\alpha H}{3C_p}. \quad (32)$$

Although the value of the upper bound $(2g\alpha H)/(3C_p)$ is not explicitly mentioned, there should be no concern regarding the forbidden situation $\eta > 1$ because H is limited. Otherwise, the Oberbeck-Boussinesq approximation does not hold because density differences cannot be ignored [12]. In fact, $g\alpha H/C_p$ should be very small according to the qualitative description in [12].

An interesting drop in efficiency occurs at $R/R_c = 25$ because $\langle Z \rangle$ drops when the dynamics become chaotic (see also [7]). An explanation of the abrupt drop in $\langle Z \rangle$ is given in the Appendix.

V. SUMMARY AND DISCUSSION

In this study, the thermodynamic efficiency of the atmospheric motion governed by the Lorenz system was determined and calculated. It is shown in Sec. III that the heat input from the hot boundary is equal to the heat output to the cold boundary because the work, which is converted from a part of the heat input, dissipates again [12].

An upper bound of the efficiency exists when the Rayleigh number R varies, which is similar to the results in [7], regardless of whether the dynamics are chaotic. The upper boundary has the same structure as that given qualitatively in [12].

For the parameter sets that can cause the dynamics to be chaotic, an abrupt drop in efficiency occurs at Hopf bifurcation. This drop, which is due to the discontinuity of $\langle Z \rangle$, is also discovered in the Malkus-Lorenz waterwheel system [7].

Thus, the efficiency determined in this study can be expressed as

$$\eta = \eta_{\max}(H) \times \eta_{\text{II}}(R(\Delta T; H)). \quad (33)$$

η_{\max} , which is defined as

$$\eta_{\max}(H) \equiv \frac{2g\alpha H}{3C_p}, \quad (34)$$

shares the same structure as in [12] (see Eq. (18)). In addition, η_{II} , which may be considered as the second-law efficiency that quantifies a ratio of the efficiency to the maximum one η_{\max} corresponding to reversible thermodynamic processes [18], exhibits properties similar to those in [7].

However, the efficiency in this study was not exactly the same as that in [7]. Both the ‘‘Rayleigh number’’ and ‘‘Prandtl number’’ are variable in the Malkus-Lorenz system by adjusting friction rate ‘‘ ν ’’ and water inflow mode, but the Prandtl number is fixed here for the specific fluid, and Rayleigh number can be changed by only adjusting ΔT . Moreover, the length scale H is limited due to the Oberbeck-Boussinesq approximation [12]. Despite these differences, such similarities are interesting. We expect that the present study contributes to the understanding of the complex climate system from the thermodynamics point of view.

ACKNOWLEDGMENTS

This work was supported by JSPS KAKENHI Grant Numbers 19K03651 and 22K03450.

Appendix: Abrupt drop of $\langle Z \rangle$

The average $\langle \cdot \rangle$ is a linear operator, and for a limited function f , it can be proven that

$$\left\langle \frac{df}{dt} \right\rangle = 0, \quad (\text{A.1})$$

$$\langle f^2 \rangle \geq 0 \quad (\text{A.2})$$

and

$$\langle f^2 \rangle \geq \langle f \rangle^2 \quad (\text{A.3})$$

with equality if and only if f is a constant.

Note that the variables in the Lorenz equations in Eq. (13) are limited because they approach a stable fixed point or evolve through a chaotic attractor [7]. Applying Eq. (A.1) to the third equation in Eq. (13) gives

$$\langle XY \rangle = b \langle Z \rangle. \quad (\text{A.4})$$

Multiplying X on both sides of the first equation in Eq. (13), and applying Eq. (A.1), we obtain

$$\langle XY \rangle = \langle X^2 \rangle. \quad (\text{A.5})$$

Therefore, the efficiency of Eq. (31) can be re-expressed as:

$$\eta \propto 1 - \frac{R}{R + 2R_c \langle Z \rangle}. \quad (\text{A.6})$$

The decrease in η at $R/R_c = \sigma(\sigma + b + 3)/(\sigma - b - 1)$ indicates an abrupt drop in $\langle Z \rangle$ at the same point.

Multiplying Y on both sides of the second equation and Z on both sides of the third equation of Eq. (13), followed by applying Eq. (A.1), gives the following

$$\begin{aligned}\langle XYZ \rangle &= r \langle XY \rangle - \langle Y^2 \rangle \\ &= rb \langle Z \rangle - \langle Y^2 \rangle,\end{aligned}\quad (\text{A.7})$$

and

$$\langle XYZ \rangle = b \langle Z^2 \rangle. \quad (\text{A.8})$$

Equation (A.3) shows $\langle Z^2 \rangle \geq \langle Z \rangle^2$ with equality if and only if the dynamics are stationary. Thus,

$$\langle XYZ \rangle \geq b \langle Z \rangle. \quad (\text{A.9})$$

Consider the following relationship:

$$\begin{aligned}0 &= \langle X - Y \rangle^2 \leq \langle (X - Y)^2 \rangle \\ &= \langle X^2 \rangle - 2 \langle XY \rangle + \langle Y^2 \rangle \\ &= -b \langle Z \rangle + \langle Y^2 \rangle,\end{aligned}\quad (\text{A.10})$$

with equality if and only if the dynamics are stationary, which implies that

$$\langle XYZ \rangle \leq (r - 1)b \langle Z \rangle. \quad (\text{A.11})$$

With Eq. (A.9) and Eq. (A.11), we obtain:

$$\langle Z \rangle^2 \leq (r - 1) \langle Z \rangle. \quad (\text{A.12})$$

For $r = R/R_c \geq 1$,

$$0 \leq \langle Z \rangle \leq r - 1. \quad (\text{A.13})$$

Note that $r - 1$ is the value of Z at fixed points (16), $\langle Z \rangle = r - 1$ when the dynamics are stationary, and $\langle Z \rangle < r - 1$ when the dynamics are chaotic. Thus, an abrupt drop in Z occurs at $R/R_c = \sigma(\sigma + b + 3)/(\sigma - b - 1)$, which is the point at which the dynamics become chaotic from stationary and leads to a drop in η at the same point (see Fig. 2).

-
- [1] B. Saltzman, *J. Atmos. Sci* **19**, 329 (1962).
 - [2] E. N. Lorenz, *J. Atmos. Sci* **20**, 130 (1963).
 - [3] N. Hemati, *Trans. Circuits Syst. I* **41**, 40 (1994).
 - [4] D. Poland, *Physica D* **65**, 86 (1993).
 - [5] S. H. Strogatz, *Nonlinear dynamics and chaos: with applications to physics, biology, chemistry, and engineering*, 2nd ed. (CRC press, 2018).
 - [6] W. V. R. Malkus, *Mem. Roy. Sci. Liège* **4**, 125 (1972).
 - [7] Á. G. López, F. Benito, J. Sabuco, and A. Delgado-Bonal, arXiv:2202.07653v2 [10.48550/arXiv.2202.07653](https://arxiv.org/abs/10.48550/arXiv.2202.07653) (2022).
 - [8] V. Lucarini, K. Fraedrich, and F. Lunkeit, *Atmos. Chem. Phys.* **10**, 9729 (2010).
 - [9] M. Ghil and V. Lucarini, *Rev. Mod. Phys.* **92**, 035002 (2020).
 - [10] M. S. Singh and M. E. O'Neill, *Rev. Mod. Phys.* **94**, 015001 (2022).
 - [11] V. Lucarini, *Phys. Rev. E* **80**, 021118 (2009).
 - [12] D. J. Tritton, *Physical fluid dynamics* (Springer Science & Business Media, 2012).
 - [13] E. N. Lorenz, *Tellus* **7**, 157 (1955).
 - [14] E. N. Lorenz, World meteorological organization **161** (1967).
 - [15] J. P. Peixoto, A. H. Oort, M. De Almeida, and A. Tomé, *Journal of Geophysical Research: Atmospheres* **96**, 10981 (1991).
 - [16] D. R. Johnson, in *International Geophysics*, Vol. 70 (Elsevier, 2000) pp. 659–720.
 - [17] W. V. R. Malkus and G. Veronis, *Journal of Fluid Mechanics* **4**, 225 (1958).
 - [18] Y. A. Cengel, M. A. Boles, and M. Kanoğlu, *Thermodynamics: an engineering approach*, 8th ed., Vol. 5 (McGraw-hill, New York, 2011).